

Preparation and Characterization of PLA/Polypyrrole Blends with Antibacterial Properties

Mônica F. B. Rocha^a, Maurício F. de Aguiar^a, Glória M. Vinhas^b, Celso P. de Melo^c,

Carolina L. Morell^a , Kleber G. B. Alves^{a*} 

^aUniversidade Federal de Pernambuco, Departamento de Engenharia Mecânica, 50670-901, Recife, PE, Brasil.

^bUniversidade Federal de Pernambuco, Departamento de Engenharia Química, 50670-901, Recife, PE, Brasil.

^cUniversidade Federal de Pernambuco, Departamento de Física, 50670-901, Recife, PE, Brasil.

Received: January 14, 2023; Revised: April 04, 2023; Accepted: May 09, 2023

We discuss the preparation of Polypyrrole and Polylactic Polyacid (PPy/PLA) based blends and the subsequent investigation of their antibacterial properties. After being molded through injection processing, the blends were characterized by Fourier transform infrared spectroscopy (FTIR), scanning electron microscopy (SEM), Impedance Spectroscopy (IS), contact angle, thermogravimetry (TGA), and dynamic mechanical analysis (DMA). FTIR analysis confirmed the presence of PPy chains and the IS results indicated that the blends prepared with a 50% mass fraction of PPy have a conductive character. While the SEM images reveal the presence of small cracks on the surface of the samples, DMA analyses show that a decrease in their mechanical strength occurs in the 50°C-60°C range, with the blend with a 50% PPy load exhibiting the greater resistance and being able to withstand temperatures of the order of 120°C. The TGA degradation profile varies according to the amount of polypyrrole present in the blends, with those containing 50% PPy being able to retain about 32% of the polypyrrole mass at 600°C. The antibacterial activity tests done with the injected blends reveal that while no inhibition halo was formed for the *Escherichia coli* bacterium, the growth of *Staphylococcus aureus* is inhibited in the 50% PPy blend.

Keywords: Polypyrrole, Polylactic acid, Extrusion, Injection, Antibacterial activity.

1. Introduction

Microbial infection or contamination is a serious problem in clinical/hospital environments, medical devices, hygiene products, water purification systems, textile materials, food packaging, and food storage. To face this, antibiotics are designed to interfere with cell synthesis, proteins, DNA, and other cellular activities¹.

Although a natural process, antibiotic resistance is becoming one of the most pressing threats to global health, due to the large-scale misuse of antibiotics in humans and animals. Many infections (such as pneumonia, salmonellosis, gonorrhea, and tuberculosis) are increasingly more difficult to treat as the most used antibiotics gradually become ineffective². Consequently, some hospital stays become longer, and larger mortality rates and higher medical costs result. The emergence of resistant bacteria has spurred intensive research in different fields, including the development of antimicrobial fabrics and packaging and the introduction of new wide-range biocides for textiles and coatings that can potentially better control and reduce the spread of antibiotic-resistant bacterial strains³.

Polymers with antibacterial properties or polymeric biocides are stable, non-volatile, and do not penetrate the skin, factors that contribute to their low cytotoxicity⁴. In its

turn, conductive polymers (CPs), such as polyaniline (PANI) and polypyrrole (PPy), have received significant attention for reuniting advantageous properties such as easy preparation, low cost, low toxicity, and biocompatibility⁵⁻⁶. Also, they have recently shown excellent antibacterial properties in textiles, with PPy deserving special mention in that regard⁶. The bioactivity of PPy seems to be associated with the presence of positive charges along the main chain, as this cationic behavior confers to them an important antibacterial action. These charges, which are a result of the polymerization process, can be stabilized by anions introduced as counterions into the polymeric matrix⁷.

Due to these properties, polypyrrole has found several applications in sensors and biosensors⁸, supercapacitors⁹, bactericidal agents¹⁰, water remediation¹¹ and disinfection¹², and food packaging¹³. PPy, which is shown to be able to inhibit methicillin-resistant *Staphylococcus aureus*¹⁴, among other bacteria, has also been used in recent years as an antimicrobial agent in textile applications¹⁵.

The use of antimicrobials is fundamental in various fields, such as the food and textile industries and medicine¹⁶. Blends and conductive composites based on PPy have found applications in the development of biofilms with antibacterial properties¹⁷ against Gram-positive and Gram-negative pathogens. Polylactic acid (PLA) is a biobased polymer suitable

*e-mail: kleber.gbalves@ufpe.br

for biomedical applications and packaging due to its good biodegradability and biocompatibility. Its potential for use in these and related areas is enhanced after the combination with polymers with antimicrobial properties, such as PPy. The characteristics of high rigidity, transparency, and easy processability, including the possibility of 3D printing, also make promising the larger use of PLA in other areas, such as in the automotive, electronics, and civil construction markets¹⁸.

The present work is aimed at the preparation of blends of PLA and PPy through melt extrusion and their subsequent molding by injection, and their characterization. These two polymers were mixed when in the molten state through extrusion and injection, two of the most used methods of processing plastics in different industrial areas. Afterward, we evaluated the antibacterial potential of the PLA/PPy blends against *Escherichia coli* and *Staphylococcus aureus* bacteria.

2. Experimental

2.1. Materials

Polylactic acid (PLA) (3D Fila, Brazil), pyrrole monomer (Sigma-Aldrich, USA), and ferric chloride hexahydrate ($\text{FeCl}_3 \cdot \text{H}_2\text{O}$) (Dinâmica (Brazil)) were used as received. The nutrient agar (European Bacteriological Agar) and bacteriological peptone were purchased from Kasvi (Brazil). The microorganisms used in the antibacterial activity tests, *Staphylococcus aureus* (ATCC 6538) and *Escherichia coli* (ATCC 11299), were provided by the Microorganism Culture Collection of the Biosciences Center of the Federal University of Pernambuco.

2.2. Polypyrrole synthesis

The Ppy synthesis was realized by the chemical polymerization of the pyrrole. For this, 450 mL of deionized water and 1.735 mL of pyrrole (25 mmol) were added to a 500 mL flask, which was stirred for 30 min at room temperature. Then, we added 50 mL of a 1.65 mol.L⁻¹ solution of ferric chloride and continued the stirring for 24 h more. The solution was then filtered, washed with deionized water, and dried in an oven for 24 h at 70°C. Afterward, the resulting solid material was macerated, and the resulting Ppy powder was stored in a desiccator¹⁹.

2.3. Blends preparation

The pure PLA films and blends containing 12.5%wt., 25.0%wt. and 50.0%wt. of Ppy were prepared through melt extrusion and then molded by injection. The extrusion was performed in a HAAKE minilab II (Thermo Scientific-Alemanha) extruder, for 10 min, at 180 °C and 80 rpm. The filaments obtained were then cut and injected on a HAAKE Minijet II (Thermo Scientific-Alemanha) under a cylinder temperature of 230°C, mold temperature of 124°C, and injection and pressurization pressures of 730 bar, for 10 s each. The films were injected into a cylindrical mold of 32mm in diameter and 6 mm in thickness.

2.4. Characterizations

Morphological analyses were carried out using a MIRA3 scanning electron microscope (TESCAN, Czech

Republic). The samples were coated with a 20 nm layer of palladium-gold using an SC7620 mini sputter coater (Quorum Technologies, UK) and placed on a double-sided carbon tape attached to the sample holder. The Fourier transform infrared attenuated total reflection (FTIR-ATR) experiments were performed using an IRTracer-100 spectrophotometer (Shimadzu, Japan), in the 4000 cm⁻¹ to 400 cm⁻¹ range. TGA analyses of the blends, and pure Ppy and PLA samples were carried out in one Star System equipment (Mettler Toledo, USA) at the 30 °C to 600 °C temperature range. Surface wettability studies were carried out by measuring the contact angle formed by the deionized water droplets on the surface of the blend. The analyses were performed using a CAM 100 contact angle meter (KSV, Finland), and the DMA experiments were carried out on a Netzsch DMA 242 E Artemis machine. The analyses were carried out in triplicate in traction mode with a 22.5mm X 6.5mm X 0.65mm sample, in the 25°C to 165°C temperature range, and adopting a heating rate of 5 °C.min⁻¹, a frequency of 1 Hz and amplitude of 5 µm. We carried out electrical impedance spectroscopy measurements to evaluate the dielectric properties of the blends. For this, the films were placed in a 12962A sample holder (Solartron, UK) with electrodes arranged in the form of parallel plates separated by a 0.110 mm distance, connected to a 1296 dielectric interface and a 1260 impedance gain-phase analyzer (Solartron, UK), under a 100 mV AC bias and a frequency of 1 Hz.

2.5. Antibacterial test

To evaluate the antibacterial activity of the blends against the Gram-negative bacteria *Escherichia coli* and Gram-positive bacteria *Staphylococcus aureus*, we used circular samples of PLA and three blends (with 12.5%wt.; 25.0%wt. and 50.0%wt. of PPy) of approximately 1 cm of diameter. For the pure PPy, the test was performed using its powder. Each sample was previously sterilized using ultraviolet irradiation for 15 min on each side and submitted to the diffusion test in a solid medium based on the standard M2-A8 (NCCLS). The Petri plates were used with the nutrient agar medium inoculated with 10⁸ CFU of bacterial suspension (0,5 on the McFarland scale). With the help of a sterilized pipette, small wells were made in the nutrient medium and filled with pure PPy, and the load blends (12.5% PPy; 25.0% PPy, and 50.0% PPy) and PLA were placed on top of the agar. Subsequently, the Petri plates were incubated in an oven for 48 hours at 35°C for the subsequent measurement of the inhibition halos.

3. Results and Discussion

The specimens obtained after the thermal process are shown in Figure 1. Visually, the specimens are black regardless of the percentage of polypyrrole load.

Polypyrrole is an amorphous polymer with a glass transition temperature of around 350 °C²⁰. Therefore, in the temperature conditions used in the extrusion and injection processes, PPy is dispersed and distributed as solid particles inside the PLA matrix. The presence of PPy oval particles can be seen in SEM images (Figure 2) for the three blend compositions prepared. A heterogeneity in particle size dispersion could be observed for all compositions, with most

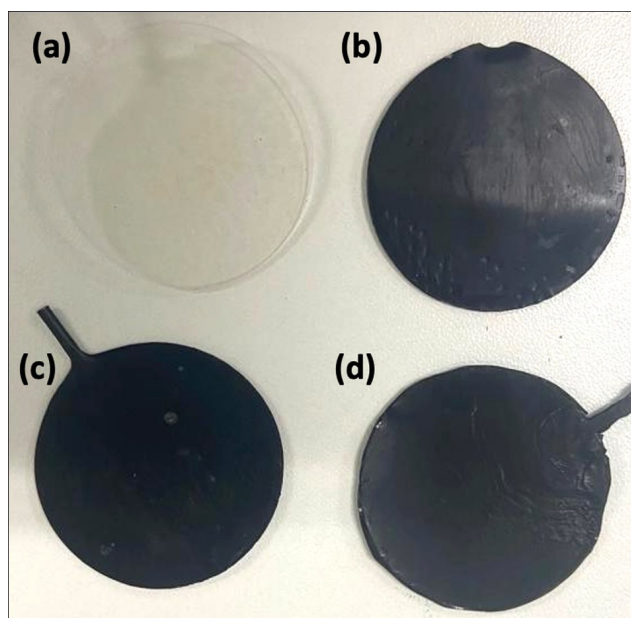


Figure 1. Blends produced PLA (a), PLA/12,5% PPy (b), PLA/25% PPy (c) and PLA/50% PPy (d).

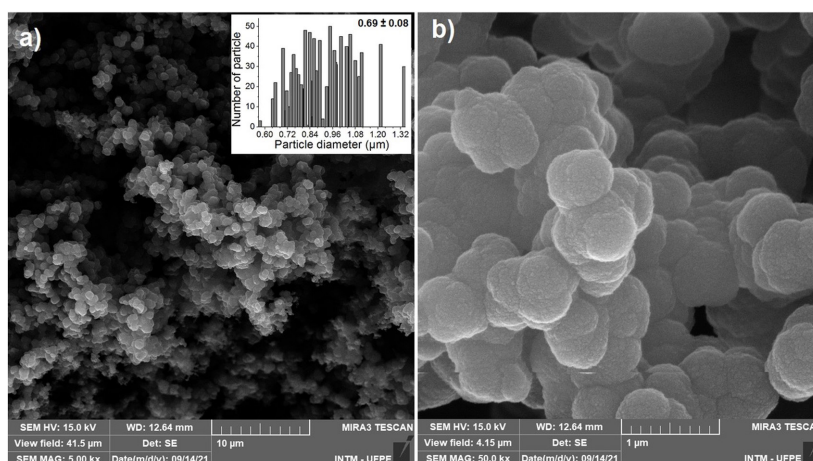


Figure 2. SEM images of PPy particles at different magnifications (a) and (b). Insets in (a) show particle size distribution of the corresponding sample.

particles having dimensions between $0.60 \mu\text{m}$ and $1.32 \mu\text{m}$. In the SEM images presented in Figure 3, one can observe the reinforcement presence of separate particles along the blend. In addition, as the percentage of PPy load increases, there is an increase in the number of agglomerates.

In the FTIR spectrum of synthesized polypyrrole (Figure 4), it was possible to observe the presence of several characteristic bands. At 1530 cm^{-1} , it is possible to observe²¹ the stretching of the C=C and C-C bonds of the polypyrrole rings. At 1297 cm^{-1} , there is a vibration band associated with the PPy rings²². Vibrations²³ due to the in-plane angular deformation of the C-H and N-H bonds are observed at 1155 cm^{-1} , and that at 1035 cm^{-1} corresponds to the =C-H deformation. As for the out-of-plane angular

deformation bands, which are related to the C-H bonds, they can be observed at 899 cm^{-1} and 776 cm^{-1} .

In the FTIR spectra of the blends (Figure 4b, 4c, and 4d), one can identify similar bands associated with PLA²⁴, referring to CH_3 symmetric vibrations, CH vibrations, C=O valence vibrations, CH deformation and asymmetric bands, CH_3 symmetrical deformation, and C-O-C asymmetric vibration and bands²⁴. The peak associated with the 1748 cm^{-1} band corresponds to the widening of the carbonyl (C=O) band. In the region where the PLA presents the bands referring to the O-C-O group, there are three peaks at 1182 , 1079 , and 1038 cm^{-1} referring to the C-C-O group. For the blends containing 12.5%wt., 25.0%wt., and 50.0%wt. of PPy, there is an overlap of the characteristic peaks of PPy at 1155 cm^{-1} , 1035 cm^{-1} , and 766 cm^{-1} .

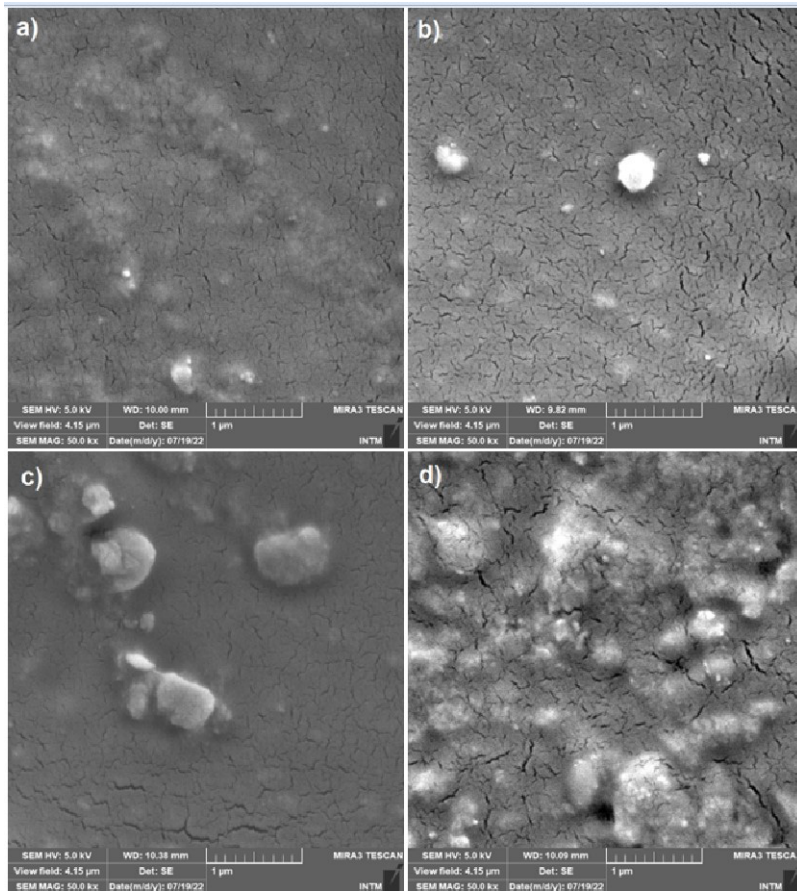


Figure 3. SEM images of PLA (a), PLA/12.5% PPy (b), PLA/25% PPy (c), and PLA/50% PPy (d).

From the impedance spectroscopy results (Figure 5), one can observe that the PLA blends with 12.5%wt. and 25.0%wt of PPy do not present conductive properties, with the data disposed of as a vertical line in the Nyquist plots, which is a characteristic of insulating materials²⁵. On the other hand, for the PLA blend with the highest PPy content (50%wt.), the data appears as a semicircle, indicating conductive properties²⁶. Therefore, a higher content of PPy was necessary for a conductive path to be formed inside the insulating PLA matrix.

In the DMA results of both PLA and the blends, presented in Figure 6, it could be seen a decrease in their storage modulus (E') in the temperature range between 50 °C and 60 °C, a fact to be expected, since this is the range where it is observed the PLA glass transition (T_g)²⁷.

For temperatures below T_g , the storage modulus of the blends was about 11% lower than that of pure PLA samples. Nonetheless, above T_g , the blend with 50%wt of PPy could still sustain a load up to 120°C and presents a storage modulus of 500 MPa at 100°C. All other samples examined had a vanishing storage modulus, i.e., do not seem able to store energy elastically. This result indicates a homogeneous distribution of PPy within the matrix, as well as a good interaction of this filler with PLA in the blend with a 50%wt composition.

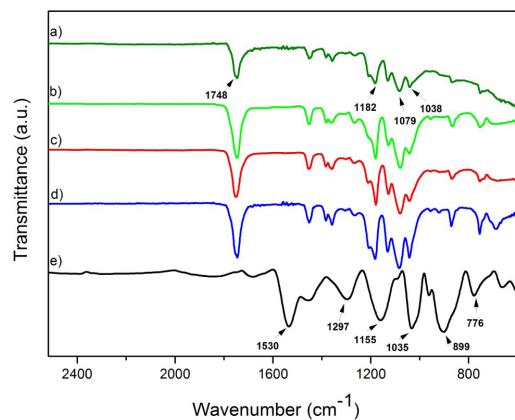


Figure 4. FTIR spectrum of PLA (a), PLA/ 12.5% PPy (b), PLA/ 25% PPy (c), PLA/ 50% PPy (d), and PPy (e).

To determine the samples' thermal degradation profile (Figure 7), the blends and the reference materials were submitted to thermogravimetric analysis (TGA). According to the expanded TGA curves, the initial mass loss in the polypyrrole curve, which is observed around 150 °C, can be

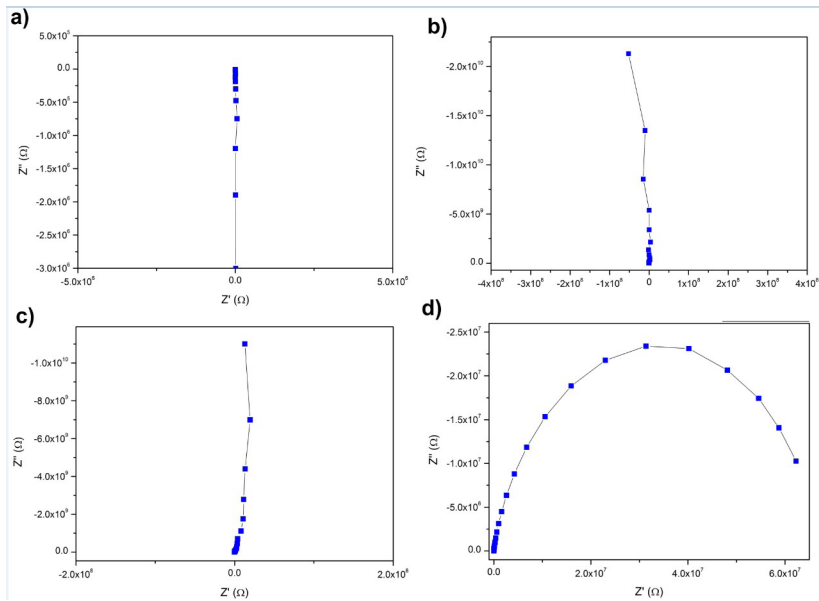


Figure 5. Impedance spectroscopy of PLA (a), PLA/PPy 12.5% (b), PLA/PPy 25% (c), and PLA/PPy 50% (d).

associated with the presence of humidity. PPy is thermally stable up to about 280 °C, when a gradual mass loss related to its degradation begins to occur, resulting in a mass residue of 60% at 600 °C.

For the TGA curve of the pure PLA films, the mass loss is observed to occur in a single step ($\Delta m = 100\%$), with the maximum degradation rate occurring at a temperature of approximately 378 °C, resulting in total PLA degradation. The thermal degradation of PLA²⁸ occurs by the random splitting of the main polymer chains, such as oxidation, polymerization, and transesterification reactions.

As for the blends, the degradation varied according to the amount of PPy filler incorporated. The TGA curve for the blend with 12.5% PPy is very similar to that of the pure PLA sample. A more significant difference is observed in the curve of the 25% blend, for which a residue of about 12% mass, due to the polypyrrole fraction, is observed. The same occurs with the 50% blend, where a polypyrrole mass of approximately 32% remains at 600°C.

The wettability of the samples was evaluated through the measurement of static water contact angles on the film surfaces. All samples exhibited contact angles (Figure 8) smaller than 90°, due to the presence of polar groups (esters) in PLA²⁹. Even though the addition of PPy in the PLA matrix increases the number of agglomerates in the composite (see Figure 2), there is no significant change in the hydrophilic behavior, since the filler is not on the surface of the films, but inside the matrix and covered by the PLA chains.

In Figure 9, we present the results relative to the antibacterial tests³⁰. For the Gram-negative *Escherichia coli*, no inhibition halo can be identified in the injected blends, with inhibition being found only in the case of the pure polypyrrole sample, where a halo with an average diameter of 1.5 cm is formed. On the other hand, the antibacterial tests of the Gram-positive *Staphylococcus aureus* bacterium

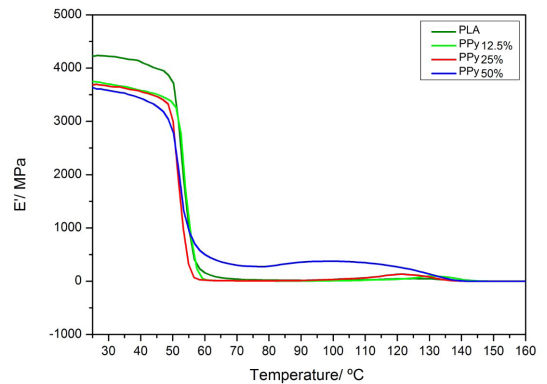


Figure 6. DMA results of PLA, PLA/12.5% PPy, PLA/25% PPy, and PLA/50% PPy.

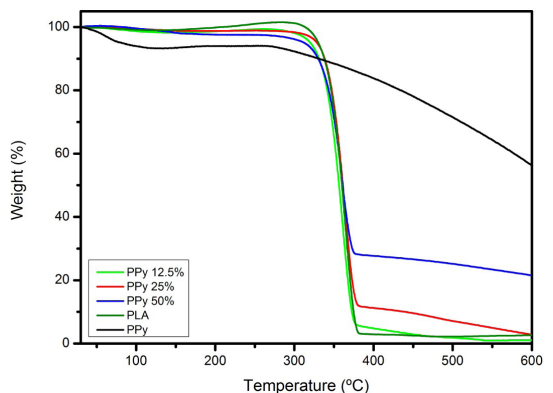


Figure 7. TGA of PLA, PLA/12.5% PPy, PLA/25% PPy, PLA/50% PPy, and PPy.

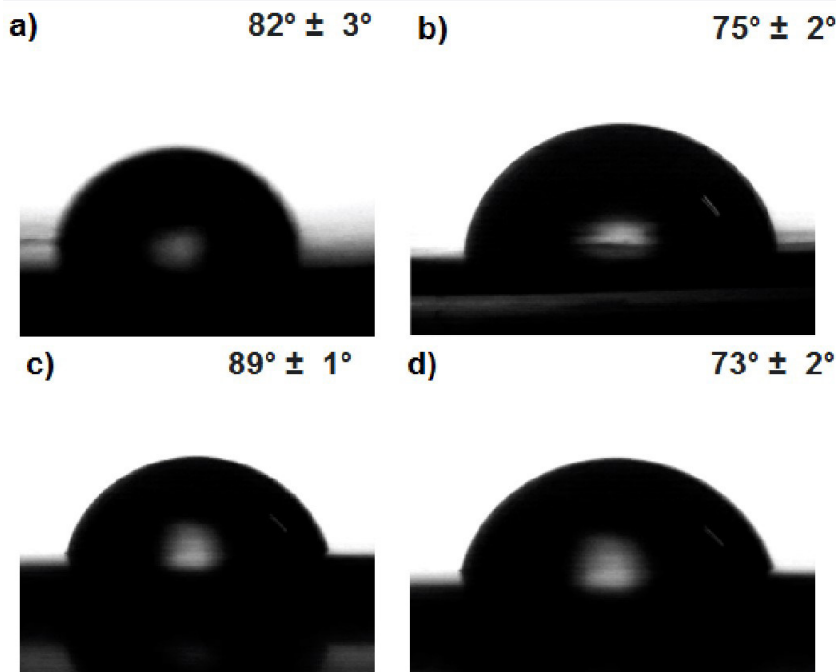


Figure 8. Contact angle PLA (a), PLA/12.5% PPy, (b), PLA/25% PPy (c), and PLA/50% PPy (d).

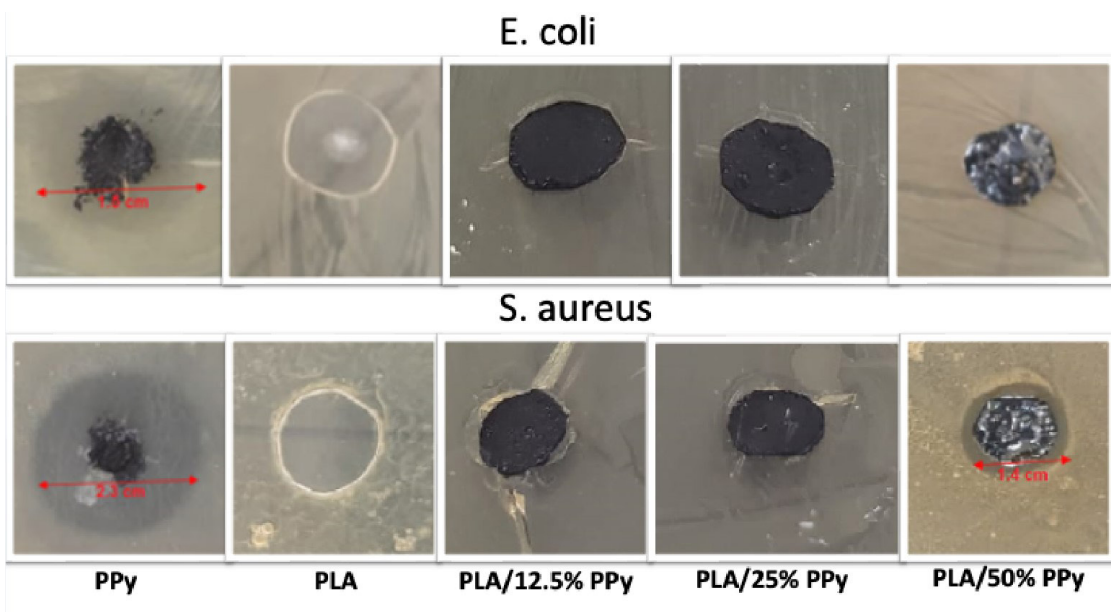


Figure 9. Halo in *Escherichia coli* and *Staphylococcus aureus* bacteria for PPy, PLA, PLA/12.5% PPy, PLA/25% PPy, and PLA/50% PPy.

indicate that there was bacterial inhibition in the blend with a 50% polypyrrole load, where a halo of 1.4 cm can be seen. As for the pure polypyrrole, in this case, an inhibition halo was formed with an average diameter of 2.3 cm. Hence, pure PPy is more effective against Gram-positive bacteria, presenting a larger inhibition halo (2.3 cm) than in the case of Gram-negative bacteria (1.5 cm). This fact explains why

the blend with 50% PPy was only effective against Gram-negative bacteria.

The bactericidal activity is attributed to the morphology of the bacterial cell³¹. Bacteria such as *S. aureus* (Gram-positive) are identified by multiple layers of peptidoglycan and a high degree of porosity, characteristics that facilitate the adsorption and diffusion of the bactericidal agent. However, the thin

wall of *E. coli* (Gram-negative) minimizes the adsorption and diffusion of bactericidal substances, and probably this characteristic of bacterial cells can favor a better efficiency of polypyrrole in inhibiting the growth of *S. aureus*. In the pertinent literature^{16,30}, one can find reports on the action of polypyrrole as a bactericide associated with the ability of this conductive polymer to interact with the surface of the bacterial cell wall through electrostatic adhesion. The mechanism proposed in Silva et al.¹⁷ suggests that the action starts with a physical interaction, which is already enough to compromise the cell metabolism, as it will impair the passive and active mechanism in energy production, and passage of nutrients and oxygen into the cell, as well as the elimination of excreta. With this change in cell permeability, there will be a reduction in biochemical reactions vital to the cell, resulting in its death.

4. Conclusion

In this work, we discussed the preparation of polylactic acid (PLA) and polypyrrole (PPy) blends through melt extrusion and molding by injection and their characterization, as well as the assessment of their antibacterial potential against the Gram-positive bacteria *Staphylococcus aureus* and the Gram-negative *Escherichia coli*. Through an EIS analysis it was observed that while the PLA/12.5% PPy and PLA/25% PPy blends do not show conductive properties, the PLA/50% PPy specimen is conductive. Our results reveal the antibacterial activity of these PLA/PPy blends, in which the inhibition of growth around the conductive sample was evident. In the test carried out with the bacterium *Escherichia coli*, only PPy showed the formation of an inhibitory halo. As for the bacterium *Staphylococcus aureus*, there was bacterial inhibition for the blend with a 50% PPy load. Therefore, it can be concluded that these blends with a higher PPy content can find promising applications in packaging and antibacterial coatings.

5. Acknowledgements

The authors acknowledge the financial support from the Brazilian agencies Coordenação de Aperfeiçoamento de Pessoal de Nível Superior - Brasil (CAPES) - Finance Code 001 and Fundação de Amparo à Ciência e Tecnologia de Pernambuco – FACEPE (Grants APQ- 0916-3.03/14).

6. References

- Maruthapandi M, Saravanan A, Gupta A, Luong JH, Gedanken A. Antimicrobial activities of conducting polymers and their composites. *Macromol.* 2022;2(1):78-99.
- Kapoor G, Saigal S, Elongavan A. Action and resistance mechanisms of antibiotics: a guide for clinicians. *J Anaesthesiol Clin Pharmacol.* 2017;33(3):300.
- Fisher JF, Meroueh SO, Mobashery S. Bacterial resistance to β -lactam antibiotics: compelling opportunism, compelling opportunity. *Chem Rev.* 2005;105(2):395-424.
- El Guerra A, Jadi SB, Bakirhan NK, Kiymani ME, Bazzaoui M, Ozkan SA et al. Antibacterial activity and volatile organic compounds sensing property of polypyrrole-coated cellulosic paper for food packaging purpose. *Polym Bull.* 2022;79:11543-66.
- Kalaiarasi J, Balakrishnan D, Al-Keridis LA, Al-Mekhlafi FA, Farrag MA, Kanisha C et al. Sensing and antimicrobial activity of polyaniline doped with TiO₂ nanocomposite synthesis and characterization. *J King Saud Univ Sci.* 2022;34:101824.
- Mowafi S, Taleb MA, El-Sayed HED. A review of plasma-assisted treatments of textiles for eco-friendlier water-less processing. *Egypt J Chem.* 2022;65(5):737-49.
- Maruthapandi M, Saravanan A, Luong JH, Gedanken A. Antimicrobial properties of polyaniline and polypyrrole decorated with zinc-doped copper oxide microparticles. *Polymers.* 2020;12(6):1286.
- Zhang D, Lang X, Hui N, Wang J. Dual-mode electrochemical biosensors based on Chondroitin sulfate functionalized polypyrrole nanowires for ultrafast and ultratrace detection of acetamidiprid pesticide. *Microchem J.* 2022;179:107530.
- Wang J, Hui N. Electrochemical functionalization of polypyrrole nanowires for the development of ultrasensitive biosensors for detecting microRNA. *Sens Actuators B Chem.* 2019;281:478-85.
- Liang W, Poon R, Zhitomirsky I. Zn-doped FeOOH-polypyrrole electrodes for supercapacitors. *Mater Lett.* 2019;255:126542.
- Mohanty N, Patra BN. Polypyrrole-sodium alginate nanocomposites for enhanced removal of toxic organic and metal pollutants from wastewater. *Mater Today Commun.* 2023;34:105325.
- Zhou Q, Huang J, Zhang X, Gao Y. Assembling polypyrrole coated sepiolite fiber as efficient particle adsorbent for chromium (VI) removal with the feature of convenient recycling. *Appl Clay Sci.* 2018;166:307-17.
- Mandu MALGMR, Costa LC, Tiosso RB, Grasso RP, Calderari MRCM. Evaluation of antimicrobial action of silver composite microspheres based on styrene-divinylbenzene copolymer. *Polímeros.* 2020;29(4):e2019052.
- Silva CFD, Oliveira FSM, Caetano VF, Vinhas GM, Cardoso SA. Orange essential oil as antimicrobial additives in poly(vinyl chloride) films. *Polímeros.* 2018;28(4):332-8.
- Majeed Z, Mushtaq M, Ajab Z, Guan Q, Mahnashi MH, Alqahtani YS et al. Rosin maleic anhydride adduct antibacterial activity against methicillin-resistant *Staphylococcus aureus*. *Polímeros.* 2020;30(2):e2020022.
- Ramirez DOS, Varesano A, Carletto RA, Vineis C, Perelshtein I, Natan M et al. Antibacterial properties of polypyrrole-treated fabrics by ultrasound deposition. *Mater Sci Eng C.* 2019;102:164-70.
- Silva FAG Jr, Vieira SA, Botton SA, Costa MM, Oliveira HP. Antibacterial activity of polypyrrole-based nanocomposites: a mini-review. *Polímeros.* 2021;30(4):e2020048.
- Balla E, Daniilidis V, Karlioti G, Kalamas T, Stefanidou M, Bikiaris ND et al. Poly (lactic acid): a versatile biobased polymer for the future with multifunctional properties—from monomer synthesis, polymerization techniques and molecular weight increase to PLA applications. *Polymers.* 2021;13(11):1822.
- Bertan A, Romio A, Brusamarello C, Domenico M. Cinética da polimerização química do pirrol em água utilizando cloreto férrico como oxidante. In: XIII Congresso Brasileiro de Engenharia Química em Iniciação Científica; 2019 Jul 21-24; Uberlândia. Proceedings. São Paulo: Blucher; 2019. p. 1-6.
- Campos RAM, Faez R, Rezende MC. Síntese do polipirrol com surfactantes aniônicos visando aplicações como absorvedores de micro-ondas. *Polímeros.* 2014;24:351-9.
- Tabačiarová J, Mičušík M, Fedorko P, Omastova M. Study of polypyrrole aging by XPS, FTIR and conductivity measurements. *Polym Degrad Stab.* 2015;120:392-401.
- Číková E, Mičušík M, Šišková A, Procházka M, Fedorko P, Omastová M. Conducting electrospun polycaprolactone/polypyrrole fibers. *Synth Met.* 2018;235:80-8.
- Chen W, Li X, Xue G, Wang Z, Zou W. Magnetic and conducting particles: preparation of polypyrrole layer on Fe₃O₄ nanospheres. *Appl Surf Sci.* 2003;218(1-4):216-22.
- Auras RA, Lim LT, Selke SE, Tsuji H. Poly (lactic acid): synthesis, structures, properties, processing, and applications. Hoboken: John Wiley & Sons; 2011.

25. Hardy CG, Islam MS, Gonzalez-Delozier D, Morgan JE, Cash B, Benicewicz BC et al. Converting an electrical insulator into a dielectric capacitor: end-capping polystyrene with oligoaniline. *Chem Mater*. 2013;25(5):799-807.
26. Oliveira AF, Santos VC, Silva LRR, Torres RG, Souza MHB. Uso da Espectroscopia de Impedância Eletroquímica (EIE) para monitoramento da corrosão em concreto com resíduo de pneu e Metacaulim e investigação da sua microestrutura. *Res Soc Dev*. 2022;11(7):e18011729826.
27. Singh B, Sharma N. Mechanistic implications of plastic degradation. *Polym Degrad Stabil*. 2007;93:561-84.
28. Minisy IM, Bober P, Acharya U, Trchová M, Hromádková J, Pflieger J et al. Cationic dyes as morphology-guiding agents for one-dimensional polypyrrole with improved conductivity. *Polymer*. 2019;174:11-7.
29. Canevarolo SV Jr. *Ciência dos polímeros: um texto básico para tecnólogos e engenheiros*. 2nd ed. São Paulo: Artliber; 2006. 280 p.
30. Varesano A, Vineis C, Aluigi A, Rombaldoni F, Tonetti C, Mazzuchetti G. Antibacterial efficacy of polypyrrole in textile applications. *Fibers Polym*. 2013;14(1):36-42.
31. Silva IDL, Oliveira FSM, Andrade MF, Brito AMSS, Hallwass F, Vinhas GM. Avaliação das potencialidades dos extratos vegetais de jurema preta (*Mimosa tenuiflora*) e cajueiro (*Anacardium occidentale* L.) para uso em embalagens ativas antimicrobianas e antioxidantes. *Matéria*. 2021;26(1):e12924.